The Journal of Immunology
RESEARCH ARTICLE | JANUARY 01 2005

Vα and Vβ Public Repertoires Are Highly Conserved in Terminal Deoxynucleotidyl Transferase-Deficient Mice[1] FREE

Nicolas Fazilleau; ... et. al

J Immunol (2005) 174 (1): 345–355.
https://doi.org/10.4049/jimmunol.174.1.345

Vα and Vβ Public Repertoires Are Highly Conserved in Terminal Deoxynucleotidyl Transferase-Deficient Mice[1]

Nicolas Fazilleau,* Jean-Pierre Cabaniols,† Fabrice Lemaître,* Iris Motta,‡ Philippe Kourilsky,* and Jean M. Kanellopoulos[2‡]

T cell repertoires observed in response to immunodominant and subdominant peptides include private, i.e., specific for each individual, as well as public, i.e., common to all mice or humans of the same MHC haplotype, Vα-Jα and Vβ-Dβ-Jβ rearrangements. To measure the impact of N-region diversity on public repertoires, we have characterized the $\alpha\beta$ TCRs specific for several CD4 or CD8 epitopes of wild-type mice and of mice deficient in the enzyme TdT. We find that V, (D), J usage identified in public repertoires is strikingly conserved in TdT$^{o/o}$ mice, even for the CDR3 loops which are shorter than those found in TdT$^{+/+}$ animals. Moreover, the 10- to 20-fold decrease in $\alpha\beta$ T cell diversity in TdT$^{o/o}$ mice did not prevent T cells from undergoing affinity maturation during secondary responses. A comparison of the CDR3β in published public and private repertoires indicates significantly reduced N-region diversity in public CDR3β. We interpret our findings as suggesting that public repertoires are produced more efficiently than private ones by the recombination machinery. Alternatively, selection may be biased in favor of public repertoires in the context of the interactions between TCR and MHC peptide complexes and we hypothesize that MHCα helices are involved in the selection of public repertoires. ***The Journal of Immunology,*** **2005, 174: 345–355.**

During thymocyte differentiation, a broad repertoire of heterodimeric $\alpha\beta$ TCRs for Ag is generated by various mechanisms (1). The somatic recombination of separate DNA segments, V and J for α-chain and V, D, and J for β-chain, yields the CDR3 of the TCR. The imprecise joining of these gene segments, the addition of template-dependent (P) and template-independent (N) nucleotides and the pairing of different α- and β-chains contribute to increase $\alpha\beta$ TCR diversity (2). Only one DNA polymerase, the nuclear enzyme TdT, catalyzes the addition of deoxynucleotide triphosphates onto the DNA 3′ OH ends in a non-germline-encoded manner, during the joining phase of the rearrangement reactions (3, 4). In the absence of TdT activity, CDR3s were shown to be shorter and less diverse (3, 5, 6). We have recently shown that 90–95% of $\alpha\beta$ TCR diversity is due to TdT and no compensatory mechanism counterbalances the decrease in diversity in TdT-deficient mice (TdT$^{o/o}$) (7). Despite this diminished TCR diversity, immune responses against viruses such as vesicular stomatitis virus and lymphocytic choriomeningitis virus (LCMV)[3] and protein Ags are unimpaired and epitope immunodominance is likewise unaltered in TdT$^{o/o}$ animals (8). T lymphocytes from TdT$^{+/+}$ and TdT$^{o/o}$ mice reacted with the same dominant epitopes of heat shock protein 65 from *Mycobacterium tuberculosis* and hen egg lysozyme (HEL) (8). When infected with the mouse pathogen LCMV or contaminated in a conventional colony by Sendai virus, TdT$^{o/o}$ mice recover from these infections. Altogether, these results indicate that TdT$^{o/o}$ animals are not immunodeficient.

T cell repertoire studies have previously shown that T cells specific for immunodominant (ID) or subdominant peptides express TCR with Vα-Jα and Vβ-Dβ-Jβ rearrangements common to all mice or humans of the same MHC haplotype (9–14). These rearrangements are referred to as public while private repertoires include those with Vα and Vβ rearrangements different from one individual to the other (9). Depending on the antigenic peptide used, one or more public rearrangements could be identified. In BALB/c mice, the T cell response against the ID HEL103–117 peptide and the subdominant HEL7–31 epitope involve a single public rearrangement for each epitope (15). Moreover, in BALB/c mice infected with LCMV, Sourdive et al. (16) have shown that 70% of CD8$^+$ T cells sorted with NP118–126 ID epitope/L^d tetramers expressed three different Vβ. In a different antigenic model, Faure et al. (17) found three public Vβ-Jβ rearrangements specific for peptide 134–148 derived from the constant region of the Ig κ L chains. In κ L chain knockout (ko) mice ($\kappa^{-/-}$) neonates born from $\kappa^{+/-}$ mothers, Cκ-specific CD4$^+$ T cells were tolerized by mother IgG. This state of tolerance was reversible and disappeared shortly after weaning, when the presentation of the Cκ peptide stopped. Interestingly, the Vβ-Jβ public repertoires against the Cκ peptide were re-expressed sequentially and the three canonical CDR3β sequences were detected at 52 wk of age in all animals, showing the high stability of public repertoire throughout life (15).

One may wonder what the driving forces are which lead to the emergence of public and private repertoires against a single epitope in primary immune responses. Two hypotheses have been put forward to explain the presence of public repertoires, i.e., higher avidity and/or higher precursor frequency as compared with

*Unité de Biologie Moléculaire du Gène-Institut National de la Santé Et de la Recherche Médicale (INSERM) Unité 277-Institut Pasteur, Paris, France; †Cellectis, Romainville, France; and ‡Laboratoire d'Activation Cellulaire et Transduction des Signaux, Institut de Biochimie et de, Biophysique Moléculaire et Cellulaire, Unité Mixte de Recherche (UMR) 8619 Centre National de la Recherche Scientifique (CNRS), Université Paris Sud, Orsay, France

Received for publication July 9, 2004. Accepted for publication October 26, 2004.

The costs of publication of this article were defrayed in part by the payment of page charges. This article must therefore be hereby marked *advertisement* in accordance with 18 U.S.C. Section 1734 solely to indicate this fact.

[1] This work is funded by INSERM, CNRS, University of Orsay and the Pasteur Institute. N.F. is supported by l'Association de Recherche contre le Cancer and by the Ministère de la Recherche. J.M.K. is supported by a grant from l'Association de Recherche contre le Cancer.

[2] Address correspondence and reprint requests to Dr. Jean M. Kanellopoulos, Laboratoire d'Activation Cellulaire et Transduction des Signaux, Institut de Biochimie et de Biophysique Moléculaire et Cellulaire, UMR 8619 CNRS, Bâtiment 430, Université Paris Sud, 91405 Orsay Cedex, France. E-mail address: Jean.Kanellopoulos@ibbmc.u-psud.fr

[3] Abbreviations used in this paper: LCMV, lymphocytic choriomeningitis virus; HEL, hen egg lysozyme; ID, immunodominant; LNC, lymph node cell; NP, nucleoprotein; HBVc, core protein of the hepatitis virus; MCC, moth cytochrome *c*; k_{off}, dissociation rate.

0022-1767/05/$02.00

private ones, no direct tests of these hypotheses have yet been performed in primary immune responses. Furthermore, it is not known whether public and private repertoire-bearing T lymphocytes fulfill different functions and/or have the same fate during secondary responses. However, Mikszta et al. (18) have shown that $CD4^+$ T lymphocytes expressing dominant pigeon cytochrome *c* clonotypes localized in the germinal centers, 9 days following immunization, while T cells bearing subdominant TCR clonotypes do not migrate significantly in the same areas. Both types of T cells were nevertheless able to enter the pool of memory cells and contributed equally to the secondary response against pigeon cytochrome *c*.

The analyses of crystal structures of the $\alpha\beta$ TCR have shown that Vα or Vβ chain forms three loops that interact with the peptide/MHC class Ia or class II molecules (reviewed in Refs. 19 and 20). These loops correspond to the CDR1 and 2 which are encoded in the Vα and Vβ genes while the CDR3 is produced by somatic recombination of V, (D), J segments. In crystal structures of most TCR-peptide-MHC class Ia complexes, CDR1 and CDR2 interact with the MHCα helices whereas the highly diverse CDR3s contact the antigenic peptide. In a recent review of the crystal structure of 15 TCR-peptide/MHC complexes, Housset and Malissen (20) have summarized some of the general features found in these complexes. In all structures, the CDR1α and CDR2α loops always interact with the MHCα2 helix even though these interactions are variable from one Vα chain to the other. A general mode of binding of the CDR1β and CDR2β to the peptide/MHC complexes is less apparent although CDR2β preferentially contacts the MHCα1 helix. The recent structural studies of a public TCR complexed to an EBV antigenic peptide bound to HLA-B8 (21) show that amino acid residues highly selected for by the recombination of the V, (D), J segments and N-addition elements contribute to the fine specificity of this receptor. Additionally, they revealed a conformational change at the N-derived residue Pro^{93} in the CDR3α which was not observed in the structure of the TCR without its ligand (21, 22). Importantly, the N-region-encoded residue Gln^{98} in the CDR3β interacts with the HLA-B8 α1 helix and two peptide residues (21).

In view of the major role played by TdT in generating CDR3 diversity, the question of whether or not public repertoires are selected for after TdT fine tuning of the TCRs seemed to us quite relevant. To test this hypothesis, we have compared the Vα and Vβ public repertoires of $TdT^{+/+}$ and $TdT^{o/o}$ mice immunized with CD4 and CD8 T cell epitopes. We found that the V, (D), J usage observed in public repertoire is strikingly conserved in $TdT^{o/o}$ mice and that T lymphocytes bearing TCR lacking N diversity can undergo affinity maturation. These findings are discussed in the context of the interactions between TCR and MHC peptide complexes.

Table I. *CDR3β sequences from HBVc-specific T cells in wild-type and $TdT^{o/o}$ animals (Vβ11-Jβ2.7 rearrangement)*

Background	CDR3 Length	3′ Vβ End	N/P/Dβ	5′ Jβ Beginning	Deduced Amino Acid Sequences	Frequency (%)[a]
C57BL/6 no. 1	7	tgtgcaagcagctta	caggca[b]	tatgaacag	**SLQAYEQ**	50
	7	tgtgcaagcagctta	gggggatggg	aacag	**SLGGWEQ**	12.5
	9	tgtgcaagcagcttag	gactgcact	cctatgaacag	SLGLHSYEQ	25
	9	tgtgcaagcagcttag	ttgggggggcgcga	gaacag	SLVGGAREQ	12.5
C57BL/6 no. 2	9	tgtgcaagcagctta	acagccct	ctcctatgaacag	SLTALSYEQ	44
	9	tgtgcaagcagcttag	taggga	gctcctatgaacag	SLVGSSYEQ	33
	9	tgtgcaagcagcttag	tgacagga	tcctatgaacag	SLVTGSYEQ	11
	9	tgtgcaagcagctta	cggactgggggt	tatgaacag	SLRTGGYEQ	11
C57BL/6 no. 3	7	tgtgcaagcagctta	cagaca	tatgaacag	**SLQTYEQ**	77.5
	9	tgtgcaagcagcttag	ctgggggggt	ctatgaacag	SLAGGVYEQ	15
	9	tgtgcaagcagc	cactgggggga	gctcctatgaacag	SHWGSSYEQ	7.5
C57BL/6 no. 4	7	tgtgcaagcagc	cgacagg	cctatgaacag	SRQAYEQ	49
	7	tgtgcaagcagctta	caggct	tatgaacag	**SLQAYEQ**	22
	7	tgtgcaagcagc	ttagggggg	ctatgaacag	**SLGGYEQ**	5
	9	tgtgcaagcagc	ctaactgggggggc	cctatgaacag	*SLTGGPYEQ*	19
	9	tgtgcaagcagctt	ggcaggaa	gctcctatgaacag	SLAGSSYEQ	5
C57BL/6 no. 5	7	tgtgcaagcagc	cccgcagggg	atgaacag	SPAGDEQ	12
	7	tgtgcaagcagcttag	gtgg	ctatgaacag	**SLGGYEQ**	6
	9	tgtgcaagcagctt	gactgggggggc	cctatgaacag	*SLTGGPYEQ*	53
	9	tgtgcaagcagctt	gaggggga	gctcctatgaacag	SLRGSSYEQ	23
	9	tgtgcaagcagctta	agtctgggggg	ctatgaacag	SLSLGGYEQ	6
$TdT^{o/o}$ no. 1	7	tgtgcaagcagctt	cgggaca	tatgaacag	SFGTYEQ	50
	7	tgtgcaagcagcttaga	tca	ctatgaacag	SLDHYEQ	50
$TdT^{o/o}$ no. 2	7	tgtgcaagcagctta	cagg	cctatgaacag	**SLQAYEQ**	92
	7	tgtgcaagcagcttag	gacaggg	tgaacag	SLGQGEQ	8
$TdT^{o/o}$ no. 3	7	tgtgcaagcagctta	cagg	cctatgaacag	**SLQAYEQ**	93
	7	tgtgcaagcagcttaga	cagggg	tgaacag	SLDRGEQ	3.5
	7	tgtgcaagcagcttag	gacaggg	tgaacag	SLGQGEQ	3.5
$TdT^{o/o}$ no. 4	7	tgtgcaagcagctta	cagg	cctatgaacag	**SLQAYEQ**	94
	7	tgtgcaagcagcttaga	ca	cctatgaacag	SLDTYEQ	2
	7	tgtgcaagcagcttaga	tggggg	tgaacag	SLDGGEQ	2
	7	tgtgcaagcagct	caggggg	ctatgaacag	SSGGYEQ	2
$TdT^{o/o}$ no. 5	7	tgtgcaagcagctta	cagg	cctatgaacag	**SLQAYEQ**	100
C57BL/6 no. 1[c]	7	tgtgcaagcagct	tgcagata	tatgaacag	**SLQIYEQ**	
C57BL/6 no. 2[c]	7	tgtgcaagcagct	taggaggtg	atgaacag	**SLGGDEQ**	

[a] Sequence occurence per total number of sequences, shown as a percentage number.
[b] Underlined nucleotides are added by TdT.
[c] Hybridomes from LNC.

Materials and Methods

Animals

All mice used in this study were 6-wk-old TdT$^{o/o}$ (C57BL/6 background) (3) or C57BL/6 mice raised in specific pathogen-free conditions and obtained from the Pasteur Institute housing facilities and Charles River Laboratories, respectively.

Peptides

NP366–74 (ASNENMETM), Eα52–66 3Kp (ASFEAQKAKANKAVD), HBVc129–40 (PPAYRPPNAPIL) were produced by NEOSYSTEM. Their purity was tested by HPLC.

Immunizations and cell cultures

Mice were immunized in the hind footpads with 10 nmol of HBVc129–140 peptide or Eα52–66 3Kp in CFA. Nine days later, popliteal lymph nodes were collected, and lymph node cells (LNC) were cultured at 5×10^5 cells per well with different concentrations of the peptide and 5% CO_2 for 4 days. All cultures were done in HL-1 medium (Cambrex) supplemented with glutamine (2 mM). The cultures were then pulsed with 1 μCi of [^{3}H]thymidine (ICN Biomedicals) for the last 8 h of the 4-day culture.

For CD8$^+$ T cell responses, mice were immunized in quadriceps muscles with 50 μg of DNA plasmid (pCI mammalian expression vector; Promega) encoding the nucleoprotein (NP) of influenza virus (strain A/PR8/34). Fourteen days later, splenocytes were collected, depleted of B220$^+$ cells and cultured at 5×10^6 cells per well with 2.5×10^5 dendritic cells previously loaded with the ID epitope of the NP (NP366–74) and 5% CO_2 for 5 days. Then, a cytotoxic assay was performed as described elsewhere (23).

Abs and sorting of cells

CD11c and B220 beads were from Miltenyi Biotec, FITC-CD4 and FITC-CD8 mAbs were from BD Pharmingen, D^b-NP366–74 MHC class I molecule tetramers were produced as described elsewhere (24, 25) and I-A^b Eα52–66 3Kp MHC class II molecule tetramers were a gift from Drs. J. Kappler and P. Marack (Department of Immunology, Howard Hughes Medical Institute, Denver, CO) and were prepared as described (26). In both cases, biotinylated complexes were mixed with PE-labeled UltraAvidin (Leinco Technologies).

Dendritic cells were prepared from spleen of wild-type mice. Cells were treated with collagenase IV (Sigma-Aldrich) and DNase (Sigma-Aldrich) and stained at 4°C for 20 min using CD11c-MACS beads. The positive fraction was purified using AUTOMACS (Miltenyi Biotec). Splenocytes from mice were depleted of B220$^+$ cells using beads and AUTOMACS. B220-negative splenocytes were incubated with indicated Abs at 4°C for 1 h, and washed. Cells were sorted on an Epics-Elite ESP (Beckman Coulter) at the Flow Cytometry Unit (Institut Jacques Monod, Paris, France). Cell purity after sorting was analyzed by flow cytometry and was above 96% in all samples.

RNA extraction and cDNA synthesis

Unfractionated or sorted T lymphocytes from TdT$^{o/o}$ and C57BL/6 mice were used for RNA preparation. Total RNA from splenocytes was extracted using an RNeasy minikit from Qiagen and reverse-transcribed into cDNA using oligo(dT) and SuperScript II (Invitrogen Life Technologies).

Immunoscope analyses

PCR were conducted in 50 μl on 1/50 of the cDNA with 2 U of *Taq* polymerase (Promega) in the supplier's buffer. cDNA was amplified using Vα- or Vβ-specific sense primers and antisense primers hybridizing in Cα or Cβ segments. Amplified products were then used as template for an elongation reaction with fluorescent-tagged oligonucleotides (run-off reactions) as described elsewhere (27).

Cloning and sequencing of TCRBV and TCRAV rearrangements

The cloning and sequencing method has been described elsewhere (28). In more details, we used a TOPO Blunt cloning kit (Invitrogen Life Technologies). A PCR amplification was performed on cloned bacteria and was followed by a second step of elongation using an ABI PRISM Big Dye Terminator kit (Applied Biosystems). Sequencing products were then read on 96 capillaries (3700 DNA Analyzer; Applied Biosystems).

Tetramer staining and kinetics of dissociation

This was done as described by Savage et al. (29). Briefly, T splenocytes were stained at 4°C for 1 h with D^b-NP366–74 tetramer and mAb (CD8-FITC). Cells were washed and the nonlabeled anti-D^b mAb KH95 was added. Tetramer staining was evaluated at different times between 0 and 120 min after KH95 addition. The normalized fluorescence (*f*) corresponds to the total fluorescence at a given time (*Fx*) divided by the total fluorescence at the initial time point (*F0*). The total fluorescence corresponds to the sum of the fluorescence intensities of CD8$^+$D^b-NP366–74 tetramer-positive cells divided by the total number of CD8$^+$ cells. Then, the ratio *ln* (*Fx*/*F0*) is plotted vs time. For each time interval of the plots, the mean slope of an interval is estimated as the equivalent of *ln* (*fa*/*fb*)/*t*, where *fa* is the normalized fluorescence at the start of the interval, *fb* the one at the end of the interval, and *t* is the length of the interval (hour).

Results

Repertoire of HBVc peptide 129–140-specific T cells

Two strategies were used to characterize in C57BL/6 mice the repertoire of T lymphocytes specific for the peptide 129–140 of the core protein of the hepatitis virus (HBVc): 1) CD4$^+$ T cell hybridomas specific for this peptide were generated and their TCR β-chains sequenced. Two of 10 CD4$^+$ T cell hybridomas reacting with HBVc129–140 used the rearrangement Vβ11-Jβ2.7 with a CDR3 of 7 aa. The sequences of their CDR3 are as follows: SLQIYEQ and SLGGDEQ (Table I). 2) The Immunoscope method was used to identify the T cell repertoires of C57BL/6 and TdT$^{o/o}$

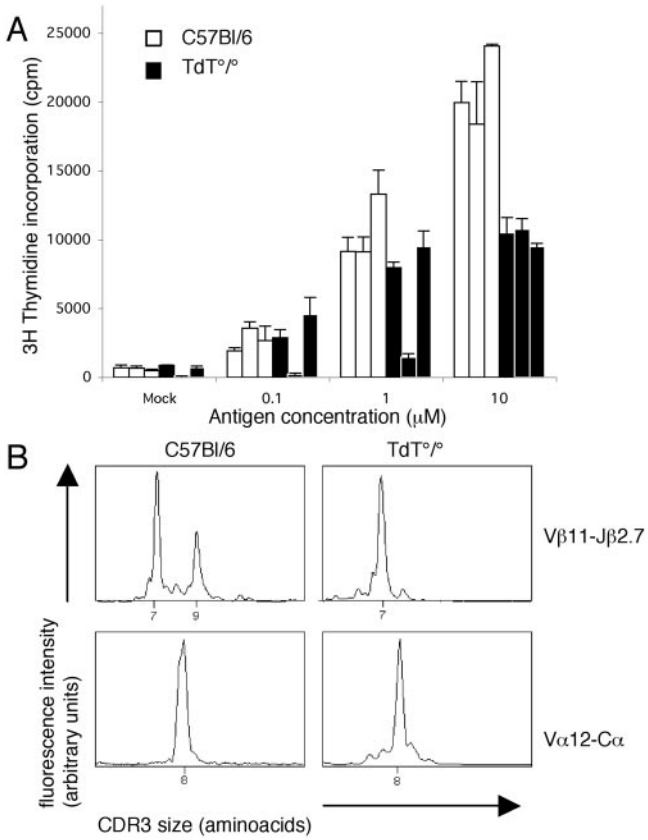

FIGURE 1. T cell response against core protein of hepatitis B virus in wild-type and TdT$^{o/o}$ animals. *A*, TdT$^{o/o}$ and wild-type mice were immunized in the hind footpads with 10 nmol of HBVc 129–140 peptide in CFA. Nine days later, LNC were cultured with increasing concentrations (μM) of HBVc 129–140 peptide for 4 days. The cultures were then pulsed with 1 μCi of [^{3}H]thymidine (TdR) for the last 8 h. Data represent TdR incorporation (cpm) from triplicate culture of three different mice. *B*, cDNA from stimulated cells was subjected to Immunoscope analyses. Data represent CDR3α and β size distributions for one representative C57BL/6 mouse and one representative TdT$^{o/o}$ mouse. Rearrangements shown are Vβ11-Jβ2.7 and Vα12-Cα. For all other Vβ11-Jβ combinations, the Immunoscope curves were bell-shaped, a characteristic of polyclonal repertoires.

mice, in response to the HBVc peptide 129–140. Briefly, the RNA extracted from in vitro HBVc peptide 129–140-stimulated LNC were reverse transcribed into cDNA, and aliquots were amplified by PCR with 24 Vβ- and Cβ-specific primers or the 21 Vα- and Cα-specific primers. The products from each PCR were then divided into aliquots and a run-off reaction was performed with the dye-labeled oligonucleotides specific for Cβ or with Cα. The fluorescent runoff products were analyzed in an automated DNA sequencer. In Cβ and Cα runoff products, we observed public expansions corresponding to peaks with CDR3 of various amino acid lengths. Every Vβ-Cβ PCR product corresponding to public expansions was divided into 12 aliquots that were hybridized with a fluorescein-labeled oligonucleotide specific for each of the 12 Jβ segments. A runoff reaction was performed and the sizes of the fluorescent runoff products were analyzed.

We immunized several animals of each strain and their LNC were challenged in vitro with increasing concentrations of HBVc peptide 129–140. After 4 days in culture, proliferative responses were measured by [^{3}H]thymidine incorporation. Animals of both strains gave maximal responses when recalled with 10 μM of peptide in vitro. However, proliferation was 2-fold higher in C57BL/6 mice at the highest concentration of Ag. In Fig. 1*A*, a typical experiment obtained with the LNC from three C57BL/6 and TdT$^{o/o}$ mice is shown.

We performed Immunoscope analyses and observed public expansions for Vβ11-Jβ2.7 rearrangements corresponding to two peaks with a CDR3 of 7 and 9 aa in C57BL/6 mice and a single peak with a CDR3 of 7 aa in TdT$^{o/o}$ animals (Fig. 1*B*, *upper panels*). Those peaks were found in all C57BL/6 mice and in four TdT$^{o/o}$ animals of five. In contrast, bell-shaped curves, characteristic of naive polyclonal repertoires, were found in the purified protein derivative controls (data not shown). Furthermore, we found a public expansion for Vα12 with a CDR3 of 8 aa in both strains of mice (Fig. 1*B*, *lower panels*).

The PCR products were cloned and sequenced. As shown in Table I (in bold letters), a CDR3 of 7 aa corresponding to the SLQAYEQ sequence was found in the Vβ11-Jβ2.7 rearrangement from 6 mice of 10. It is worth noticing that this sequence is generated without N diversity in 4 TdT$^{o/o}$ animals while it is produced with N addition in 2 C57BL/6 mice. Two CDR3 of 7 aa, coded by different nucleotidic sequences, share the same amino acid sequence (SLGGYEQ). Finally, the CDR3β sequences of two different HBVc129–140-specific T cell hybridomas are closely similar to most of the CDR3 sequences observed in different animals. The recurrent CDR3s of 9 aa are found in C57BL/6 mice only. A comparison of the 9 aa CDR3 sequences of 5 C57BL/6 shows that the CDR3 sequences of mice nos. 2, 4, and 5 reveal a consensus sequence SLXGSSYEQ; in addition, a SLXGGXYEQ consensus can be found in CDR3β sequences of animal nos. 3, 4, and 5. In C57BL/6 nos. 4 and 5, two different nucleotidic sequences generate the same CDR3, i.e., SLTGGPYEQ (in italic in Table I).

In Table II are shown the CDR3α sequences. Interestingly, the Vα12-Jα27 rearrangement is used in all C57BL/6 and four TdT$^{o/o}$ mice. It generates CDR3α with the amino acid sequence SDTNT GKL in TdT$^{o/o}$ animals while in C57BL/6 the CDR3α sequences are more diverse (in bold in Table II). However, the aspartate residue (D) in the SDTNTGKL sequence is replaced by a glutamate residue (E) (conservative mutation) in three different C57BL/6 or by a glycin residue (G) in mouse no. 2. The sequence TNTNTGKL produced by the rearrangement Vα12-Jα27 is also found in two different C57BL/6, but not TdT$^{o/o}$, animals.

In summary, it is striking that the Vα-Jα and Vβ-Jβ usage in C57BL/6 and TdT$^{o/o}$ is highly conserved in T cell responses against the HBVc peptide 129–140. Furthermore, while the 9 aa CDR3β is found in C57BL/6 mice only, the short CDR3β sequences are homologous in both strains of mice. CDR3α sequences are similar because the sequence SDTNTGKL is found in four TdT$^{o/o}$ while sequences SETNTGKL or SGTNTGKL are present in three and one C57BL/6, respectively.

Repertoire analysis of CD4$^+$ cells reactive against the Eα52–66 3K peptide in C57BL/6 and TdT$^{o/o}$ mice

The comparison between C57BL/6 and TdT$^{o/o}$ mice in terms of rearrangements used by peptide-specific CD4$^+$ T cells was extended to another antigenic system, namely the Eα52–66 3Kp which induces strong proliferative responses in C57BL/6 mice.

Table II. *CDR3α sequences from HBVc-specific T cells in wild-type and TdT$^{o/o}$ animals (Vα12-Cα rearrangement)*

Background	Jα	3′ Vα End	N/P	5′ Jα Beginning	Deduced Amino Acid Sequences	Frequency (%)[a]
C57BL/6 no. 1	27	tgtgctc	agac	taacaccaatacaggcaaatta	**TNTNTGKL**	33.5
	45	tgtgc	cccgggggg	cagaaggtgcagatagactc	GAEGADRL	33.5
	27	tgtgctttgag	g	accaatacaggcaaatta	**SETNTGKL**	22
	12	tgtgctctg	ccc	gggactggaggctataaagtg	PGTGGYKV	11
C57BL/6 no. 2	27	tgtgctctgagtg	gg	accaatacaggcaaatta	**SGTNTGKL**	88
	58	tgtgctttgag		gcaaggcactgggtctaagctg	RQGTGSKL	12
C57BL/6 no. 3	22	tgtgctctgagt	aca	tctggcagctggcaactc	STSGSWQL	66
	45	tgtgc	cccgggggg	cagaaggtgcagatagactc	GAEGADRL	17
	27	tgtgctttgag	g	accaatacaggcaaatta	**SETNTGKL**	17
C57BL/6 no. 4	22	tgtgctttg	ca	atcttctggcagctggcaactc	QSSGSWQL	30
	4	tgtgctctgag		atctggtagcttcaataagttg	RSGSFNKL	50
	27	tgtgctttgag	g	accaatacaggcaaatta	**SETNTGKL**	20
C57BL/6 no. 5	26	tgtgctctga	ccctt	aactatgcccagggatta	TLNYAQGL	60
	27	tgtgctc	agac	taacaccaatacaggcaaatta	**TNTNTGKL**	40
TdT$^{o/o}$ no. 1	27	tgtgctctgagtga		caccaatacaggcaaatta	**SDTNTGKL**	40
	30	tgtgctctgagtga		cacaaatgcttacaaagtc	SDTNAYKV	40
	4	tgtgctctgagtga		tggtagcttcaataagttg	SDGSFNKL	20
TdT$^{o/o}$ no. 2	39	tgtgctctgagt		aataatgcaggtgccaag	SNNAGAKL	100
TdT$^{o/o}$ no. 3	27	tgtgctctgagtga		caccaatacaggcaaatta	**SDTNTGKL**	100
TdT$^{o/o}$ no. 4	39	tgtgctctgagt		aataatgcaggtgccaag	SNNAGAKL	77
	27	tgtgctctgagtga		caccaatacaggcaaatta	**SDTNTGKL**	23
TdT$^{o/o}$ no. 5	27	tgtgctctgagtga		caccaatacaggcaaatta	**SDTNTGKL**	60
	26	tgtgctctgagtga	t	aactatgcccagggatta	SDNYAQGL	40

[a] Sequence occurence per total number of sequences, shown as a percentage number.

Moreover, the availability of Eα52–66 3Kp/I-A^b tetramers allows for the isolation of peptide-specific T cells (26).

Mice were immunized and 9 days later, LNC were restimulated in vitro with increasing concentrations of Eα52–66 3Kp (Fig. 2*A*). We sorted out by flow cytometry the specific $CD4^+$ T cells from LNC with Eα52–66 3Kp/I-A^b tetramers. Immunoscope analyses revealed an amplification of the rearrangement Vα7-Cα of 8 aa (Fig. 2*B*, *lower panels*). For the Vβ, we observed that, in all animals, the Vβ6-Jβ2.7 segment was amplified. The PCR products were cloned and sequenced. A CDR3β of 6 aa with the sequence SMDYEQ is found in all $TdT^{o/o}$ animals while CDR3β of 6 and 9 aa are identified in C57BL/6 mice (Table III). For the CDR3β of 6 aa the consensus sequence found in C57BL/6 is SXDYEQ and the SMDYEQ sequence is found in C57BL/6 no. 2 only (in bold in Table III). For the CDR3β of 9 aa, the consensus sequence is SXXDWGYEQ and the sequence SMGDWGYEQ is found in three C57BL/6.

In Table IV are shown the CDR3α sequences in response to Eα52–66 3Kp. All C57BL/6 mice use the Vα7-Jα13 rearrangement generating the SANSGTYQ sequence (in bold in Table IV). In two $TdT^{o/o}$ animals, the same rearrangement and CDR3α sequence are found. Surprisingly, two $TdT^{o/o}$ mice use a different rearrangement (Vα7-Jα26) even though the SANSGTYQ sequence does not contain N diversity. The Jα26 segment is also found in C57BL/6 mouse no. 2 leading to the CDR3α sequence SENYAQGL while in $TdT^{o/o}$ using the same Jα segment the CDR3α sequence is SDNYAQGL (in italic in Table IV). It is striking that in the rearrangement containing N diversity the aspartate residue (D) found in the CDR3α of the $TdT^{o/o}$ animals is replaced by a glutamate residue (E). As observed for the HBVc peptide 129–140, the Vα-Jα and Vβ-Jβ usage in T cell responses against the Eα52–66 3Kp is highly conserved and the CDR3 sequences are homologous in both strains of mice. In addition, we found, by quantitative PCR on tetramer-positive T lymphocytes, that the percentages of Eα52–66 3Kp-specific Vα7 segment were similar in both strains of mice i.e., 16.3 ± 2.4% in C57BL/6 vs 18.8 ± 5.5% in $TdT^{o/o}$ (four mice for each group).

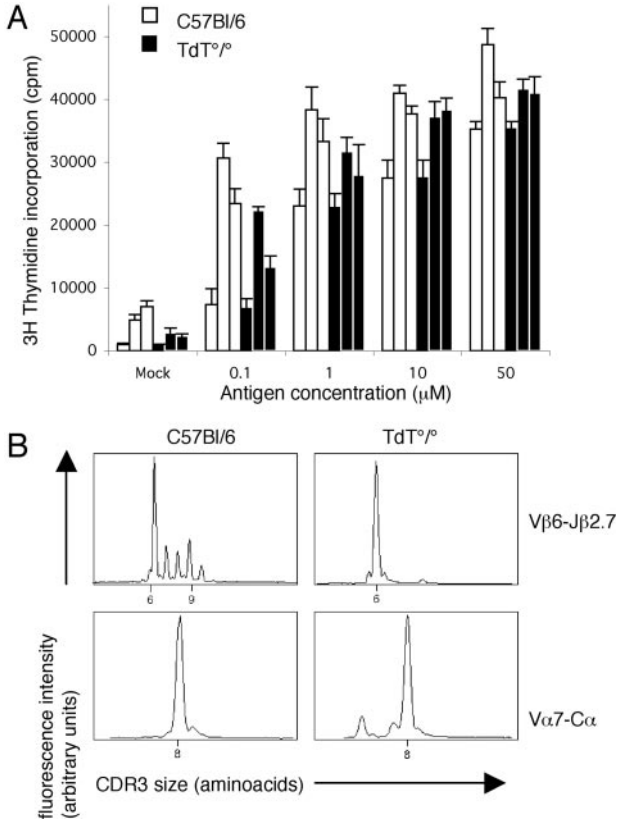

FIGURE 2. T cell response against peptide Eα52–66 3Kp in wild-type and $TdT^{o/o}$ animals. *A*, $TdT^{o/o}$ and wild-type mice were immunized in the hind footpads with 10 nmol of Eα52–66 3Kp peptide in CFA. Nine days later, LNC were cultured with increasing concentrations (μM) of Eα52–66 3Kp peptide for 4 days. The cultures were then pulsed with 1 μCi of [^{3}H]thymidine (TdR) for the last 8 h. Data represent TdR incorporation (cpm) from triplicate culture of three different mice. *B*, Mice were immunized like in *A*. Nine days after, $CD4^+$ I-A^b Eα 52–66 3Kp-positive cells were sorted out using flow cytometry (at least 97% of purity). cDNA from these cells was subjected to Immunoscope analyses. Data represent CDR3α and β size distribution for one representative C57BL/6 mouse and one representative $TdT^{o/o}$ mouse. Rearrangements shown are Vβ6-Jβ2.7 and Vα7-Cα.

Repertoires of $CD8^+$ T cells specific for the immunodominant peptide of the NP of influenza virus in C57BL/6 and $TdT^{o/o}$ mice

The repertoire of $CD8^+$ T cells generated in response to the ID peptide of the NP of influenza virus (NP366–74) was next identified. This antigenic model presents the advantage that peptide-specific T lymphocytes can be purified using NP366–74/H-2 D^b tetramers.

Mice were immunized with 50 μg of plasmid encoding the NP of influenza virus. Fourteen days later, splenocytes were cultured for 5 days in the presence of NP366–74 peptide-pulsed dendritic cells and their cytotoxic activity was tested (Fig. 3). T cells from both C57BL/6 and $TdT^{o/o}$ mice are efficient in killing peptide-pulsed target cells and no significant statistical difference between the two mouse strains was observed. NP366–74 peptide-specific cells were then sorted out from spleens of immunized mice, following staining with the NP366–74/H-2 D^b tetramers. Vα and Vβ T cell repertoire analyses are shown in Fig. 3*B*. For both strains of mice, an oligoclonal expansion of the Vβ8.3-Jβ2.2 of 9 aa length is observed (Fig. 3*B*, *upper panels*) while oligoclonal expansions of the Vα16 with a CDR3 length of 10 and 8 aa are found in C57BL/6 and $TdT^{o/o}$, respectively (Fig. 3*B*, *lower panels*). In Tables V and VI are shown the CDR3α and β sequences. All $TdT^{o/o}$ mice use the CDR3β sequence SGGANTGQL, while four C57BL/6 mice use preferentially the CDR3β sequence SGGSNT GQL and one animal the sequence SGGGNTGQL (Table V, in bold). Overall, the consensus sequence for both strains of mice is SGGXNTGQL. It is worth noticing that in $TdT^{o/o}$ no. 3, the sequence SGGANTGQL is mainly generated by germline nucleotidic sequence while, in 4% of the bacterial clones sequenced, it is produced with a single P addition.

All $TdT^{o/o}$ mice use preferentially Vα16-Jα15, the same CDR3 RDQGGRAL is found with the highest frequency in the bacterial clones sequenced (Table VI, in bold). Another sequence RANS GTYQ is found in $TdT^{o/o}$ mice nos. 1 and 4. This sequence is generated by the Vα16-Jα13 rearrangement. However, all wild-type mice use the Vα16-Jα42 with a longer CDR3 (10 aa). The consensus sequence is RXSGGSNAKL. It is interesting to note that beside this rearrangement, the Vα16-Jα15 combination found in all $TdT^{o/o}$ mice is also used by three C57BL/6 animals of four. Interestingly, in C57BL/6 mouse no. 2 the sequence RDQGGRAL is observed as in $TdT^{o/o}$ mice while for the other two mice the Vα16-Jα15 rearrangements are longer by two residues.

From these results, we conclude that two Vα-Jα public rearrangements (Vα16-Jα42 and Vα16-Jα15) are observed in C57BL/6 animals while a single public rearrangement (Vα16-Jα15) is used in $TdT^{o/o}$ mice. As far as the Vβ chain is concerned, there is a conservation of the Vβ-Jβ combination and the CDR3β

Table III. *CDR3β sequences from Eα52–66-specific T cells sorted out from wild-type and TdT$^{o/o}$ animals (Vβ6-Jβ2.7 rearrangement)*

Background	CDR3 Length	3′ Vβ End	N/P/Dβ	5′ Jβ Beginning	Deduced Amino Acid Sequences	Frequency (%)[a]
C57BL/6 no. 1	6	tgtgccagcagta	cagat[b]	tatgaacag	**STDYEQ**	54
	6	tgtgccagcagtat	tacag	atgaacag	SITDEQ	15
	9	tgtgccagcagtat	gggggactggggt	tatgaacag	**SMGDWGYEQ**	16
	9	tgtgccagcag	ctgggactgggggga	ctatgaacag	SWDWGDYEQ	15
C57BL/6 no. 2	6	tgtgccagcagt	tgggat	tatgaacag	SWDYEQ	60
	6	tgtgccagcagtat	gga	ctatgaacag	**SMDYEQ**	4
	6	tgtgccagcagtat	tttgg	atgaacag	SILDEQ	4
	9	tgtgccagcagta	gcggggactgggggag	tgaacag	SSGDWGSEQ	16
	9	tgtgccagcagtata	cgggactggggg	tatgaacag	SIRDWGYEQ	16
C57BL/6 no. 3	6	tgtgccagcagta	cagat	tatgaacag	**STDYEQ**	67
	6	tgtgccagcagt	ccaga	ctatgaacag	SPDYEQ	10
	6	tgtgccagcagtat	cgggg	atgaacag	SIGDEQ	3
	9	tgtgccagcagtat	gggggactgggg	ctatgaacag	**SMGDWGYEQ**	20
C57BL/6 no. 4	6	tgtgccagcagtata	at	ctatgaacag	SIIYEQ	30
	9	tgtgccagcagtat	gggggactgggg	ctatgaacag	**SMGDWGYEQ**	70
TdT$^{o/o}$ no. 1	6	tgtgccagcagtat	gga	ctatgaacag	**SMDYEQ**	100
TdT$^{o/o}$ no. 2	6	tgtgccagcagtat	gga	ctatgaacag	**SMDYEQ**	82
	6	tgtgccagcagtat	gggg	tatgaacag	SMGYEQ	18
TdT$^{o/o}$ no. 3	6	tgtgccagcagtat	gga	ctatgaacag	**SMDYEQ**	91
	6	tgtgccagcagta	caggg	tatgaacag	STGYEQ	9
TdT$^{o/o}$ no. 4	6	tgtgccagcagtat	gga	ctatgaacag	**SMDYEQ**	100

[a] Sequence occurence per total number of sequences, shown as a percentage number.
[b] Underlined nucleotides are added by TdT.

from C57BL/6 differs from those of TdT$^{o/o}$ by A vs G or S (Table V) only. As in the previous paragraph, we have assessed by quantitative PCR on isolated tetramer-positive T lymphocytes the percentages of NP366–74-specific Vα16 usage. The values obtained were similar and averaged 48.2 ± 10.6% in C57BL/6 and 43.6 ± 7.9% in TdT$^{o/o}$ (four mice for each group).

Avidity and dissociation kinetics of NP-peptide/H-2D^b tetramers bound to specific CD8$^+$ splenocytes

Several groups have demonstrated that secondary T cell responses use a more focused repertoire than primary responses (29–31), a consequence of the preferential selection and expansion of T lymphocytes bearing TCR with the highest affinity. This raises the possibility that the decrease in TdT$^{o/o}$ T cell repertoire diversity may lead to an absence of affinity maturation process. To verify this hypothesis, we compared the dissociation kinetics of NP-peptide/H-2 D^b tetramers bound to CD8$^+$ splenocytes from primary and secondary responses of C57BL/6 and TdT$^{o/o}$ mice as described by Savage et al. (29). In Fig. 4*A* the schedule of immunization with the pCI-NP plasmid encoding the full-length NP of influenza virus and the pCI plasmid as a control is shown. Briefly, mice were immunized, 14 days later the splenocytes from primary responses were collected and analyzed. For secondary responses, immunized mice were boosted 2 mo after the first immunization and splenocytes were collected 1 wk after. For primary and secondary responses, the splenocytes were incubated, at 4°C for 1 h, with NP-peptide/H-2 D^b-PE-streptavidin tetramers and an anti-CD8 mAb. An aliquot was sampled out and corresponded to T0 h. An unlabeled anti-H-2 D^b mAb was added to the remaining cells at 4°C and aliquots were collected at different times. The anti-H-2 D^b was used in excess as compared with H-2 D^b molecules borne by T cells to inhibit binding of dissociated tetramers during our analysis. In Fig. 4*B* is shown a typical experiment, 2.65% tetramer-positive CD8$^+$ T lymphocytes are observed whereas only 0.09% are observed in a control mouse. The percentage of tetramer-positive CD8$^+$ T cells in C57BL/6 and TdT$^{o/o}$ animals during the

Table IV. *CDR3α sequences from Eα52–66-specific T cells sorted out from wild-type and TdT$^{o/o}$ animals (Vα7-Cα rearrangement)*

Background	Jα	3′ Vα End	N/P	5′ Jα Beginning	Deduced Amino Acid Sequences	Frequency (%)[a]
C57BL/6 no. 1	13	tgtgcagctagtg		caaattctgggacttaccag	**SANSGTYQ**	58
	15	tgtgcag	ttagtgg	ccagggaggcagagctctg	SGQGGRAL	42
C57BL/6 no. 2	13	tgtgcagctagtg		caaattctgggacttaccag	**SANSGTYQ**	62
	26	tgtgcagctagtga	a	aactatgcccagggatta	*SENYAQGL*	28
	33	tgtgcagctag	gtca	gatagcaactatcagttg	RSDSNYQL	10
C57BL/6 no. 3	21	tgtgcagctag	ggg	gtctaattacaacgtgctt	RGSNYNVL	82
	13	tgtgcagctagtg		caaattctgggacttaccag	**SANSGTYQ**	18
C57BL/6 no. 4	15	tgtgcagt	tagtgagcat	ggaggcagagctctg	SEHGGRAL	67
	13	tgtgcagctagtg	t	aaattctgggacttaccag	SVNSGTYQ	33
TdT$^{o/o}$ no. 1	26	tgtgcagctagtga		taactatgcccagggatta	*SDNYAQGL*	72
	13	tgtgcagctagtg		caaattctgggacttaccag	**SANSGTYQ**	28
TdT$^{o/o}$ no. 2	7	tgtgcagctagtga		ctacagcaacaacagactt	SDYSNNRL	100
TdT$^{o/o}$ no. 3	26	tgtgcagctagtga		taactatgcccagggatta	*SDNYAQGL*	94
	31	tgtgcagctagtg		ggaatagcaataacagaatc	SGNSNNRI	6
TdT$^{o/o}$ no. 4	13	tgtgcagctagtg		caaattctgggacttaccag	**SANSGTYQ**	55
	31	tgtgcagctagtg		ggaatagcaataacagaatc	SGNSNNRI	45

[a] Sequence occurence per total number of sequences, shown as a percentage number.

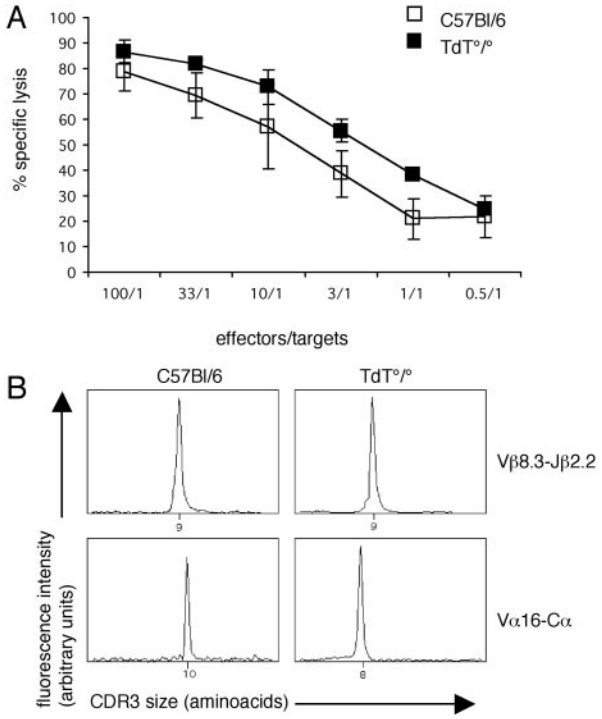

FIGURE 3. T cell response against NP of influenza virus in wild-type and TdT$^{o/o}$ animals. *A*, Mice were immunized in quadriceps muscles with 50 μg of DNA plasmid encoding the NP of influenza virus. Fourteen days later, splenocytes were cultured with 2.5×10^5 dendritic cells loaded with the ID epitope of the NP (NP 366–74) for 5 days. Then, stimulated splenocytes were tested for cytotoxicity on ^{51}Cr-labeled RMAS-NP 366–74 or RMAs target cells in 4-h ^{51}Cr release assay. The means of specific lysis from eight mice per group are presented. *B*, Moreover, stimulated CD8$^+$ D^b-NP 366–74 tetramer-positive cells were sorted out to extract their RNA. It was reverse-transcribed into cDNA. Then, Immunoscope analyses were performed as described elsewhere. Profiles of the Vβ8.2-Jβ2.2 and Vα16-Cα rearrangements are presented for one representative C57BL/6 and one representative TdT$^{o/o}$ mouse.

primary and secondary responses is presented in Fig. 4*C*. In both mouse strains, tetramer-positive CD8$^+$ cells represent between 2 and 3% of CD8$^+$ cells and this number is not significantly different in primary or secondary responses. The mean fluorescence intensities observed in primary and secondary responses were similar in C57BL/6 and TdT$^{o/o}$ mice (Fig. 4*C*). Tetramer staining decay kinetics show significant differences between primary and secondary responses in C57BL/6 as well as in TdT$^{o/o}$ mice (Fig. 5, *A* and *B*). This may indicate that, in secondary responses, T cell mean avidity is increased as compared with primary responses. Interestingly, comparison of the dissociation rate (k_{off}) at early time points (0–20 min) shows a faster k_{off} in C57BL/6 primary responses while at other time intervals the dissociation rate is almost identical for primary and secondary responses. In TdT$^{o/o}$, faster k_{off} are observed in primary responses between 0 and 40 min, at later times the k_{off} in primary and secondary responses are not statistically different. As suggested by Savage et al. (29), these results may be indicative of the presence in primary responses of subsets of T lymphocytes bearing TCR with the highest k_{off} for their ligands. In secondary responses, these T cells are outcompeted by T lymphocytes bearing TCR with lower k_{off} for their ligands.

The results shown in Fig. 5 are statistically significant and each group corresponds to five mice. Surprisingly, we did not observe, in the anti-NP peptide CD8 T cell responses, the large variations in tetramer staining decay found from mouse to mouse in the response to moth cytochrome *c* (MCC)/I-E^k complexes (29).

Comparison of the number of N nucleotides present in the CDR3β of public and private rearrangements

Several non-mutually exclusive explanations underlie the extraordinary stability over time (15) and the favored selection of public repertoires: 1) public repertoires are generated more easily than private ones by the recombination machinery; 2) public repertoires which contain few N nucleotides are more efficiently selected for by MHC molecules during thymic selection; and 3) private repertoires bearing more N nucleotides in their CDR3 are selected by peptide/MHC complexes but they have a better fit for the aa residue side chains of the self-peptide.

In Table VII are shown statistical analyses of the numbers of N nucleotides in the CDR3β of published public and private repertoires. We found a statistically significant difference between the number of N nucleotides contained in CDR3β of public vs private rearrangements (1.64 vs 3.09 N nucleotides, $p < 0.001$). The same analysis for the CDR3α could not be performed because the numbers of public vs private Vα repertoires available are insufficient.

Table V. *CDR3β sequences from influenza virus NP-specific T cells sorted out from wild-type and TdT$^{o/o}$ animals (Vβ8.3-Jβ2.2 rearrangement)*

Background	3′ Vβ End	N/P/Dβ	5′ Jβ Beginning	Deduced Amino Acid Sequences	Frequency (%)[a]
C57BL/6 no. 1	tgtgccagcagtg	gggggggg[b]	aacaccgggcagctc	**SGGGNTGQL**	62.5
	tgtgccagcagtg	gaggggg	aaacaccgggcagctc	**SGGGNTGQL**	37.5
C57BL/6 no. 2	tgtgccagc	tcaggggtt	caaacaccgggcagctc	**SGGSNTGQL**	54.9
	tgtgccagcagtg	ggggct	caaacaccgggcagctc	**SGGSNTGQL**	45.1
C57BL/6 no. 3	tgtgccagcagtg	gaggggg	aaacaccgggcagctc	**SGGGNTGQL**	79.5
	tgtgccagcagtg	gagggggg	aacaccgggcagctc	**SGGGNTGQL**	2.3
	tgtgccagcagtg	ggggat	caaacaccgggcagctc	**SGGSNTGQL**	18.2
C57BL/6 no. 4	tgtgccagcagtg	ggggtt	caaacaccgggcagctc	**SGGSNTGQL**	88.8
	tgtgccagca	agggggggg	caaacaccgggcagctc	KGGANTGQL	9.8
	tgtgccagc	ggtgggggtt	caaacaccgggcagctc	GGGSNTGQL	1.4
TdT$^{o/o}$ no. 1	tgtgccagcagtg	gggggg	caaacaccgggcagctc	**SGGANTGQL**	100
TdT$^{o/o}$ no. 2	tgtgccagcagtg	gggggg	caaacaccgggcagctc	**SGGANTGQL**	100
TdT$^{o/o}$ no. 3	tgtgccagcagtg	gggggg	caaacaccgggcagctc	**SGGANTGQL**	96
	tgtgccagcagtg	ggggggcg	aacaccgggcagctc	**SGGANTGQL**	4
TdT$^{o/o}$ no. 4	tgtgccagcagtg	gggggg	caaacaccgggcagctc	**SGGANTGQL**	100

[a] Sequence occurence per total number of sequences, shown as a percentage number.
[b] Underlined nucleotides are added by TdT.

Table VI. *CDR3α sequences from influenza virus NP-specific T cells sorted out from wild-type and TdT$^{o/o}$ animals (Vα16-Cα rearrangement)*

Background	Jα	CDR3 Length	3′ Vα End	N/P	5′ Jα Beginning	Deduced Amino Acid Sequences	Frequency (%)[a]
C57BL/6 no. 1	15	10	tgtgctatgagag	cgg	cctaccagggaggcagagctctg	RAAYQGGRAL	61
	42	10	tgtgctatgagag	gt	tctggaggaagcaatgcaaagcta	**RGSGGSNAKL**	29.5
	42	10	tgtgctatgag	gagaggg	ggaggaagcaatgcaaagcta	RRGGGSNAKL	9.5
C57BL/6 no. 2	15	8	tgtgctatgagaga		ccagggaggcagagctctg	**RDQGGRAL**	96
	42	10	tgtgctatgagag	gt	tctggaggaagcaatgcaaagcta	**RGSGGSNAKL**	4
C57BL/6 no. 3	42	10	tgtgctatgagag	tc	tctggaggaagcaatgcaaagcta	**RVSGGSNAKL**	83
	15	10	tgtgctatgagag	cgg	cctaccagggaggcagagctctg	RAAYQGGRAL	17
C57BL/6 no. 4	34	10	tgtgctatgagagag	cca	tcttccaataccaacaaagtc	REPSSNTNKV	69
	42	10	tgtgctatgagagag		tctggaggaagcaatgcaaagcta	**RESGGSNAKL**	31
TdT$^{o/o}$ no. 1	15	8	tgtgctatgagaga		ccagggaggcagagctctg	**RDQGGRAL**	49
	13	8	tgtgctatgagag		caatttctgggacttaccag	RANSGTYQ	30
	13	8	tgtgctatgagagaggg	c	tctgggacttaccag	REGSGTYQ	21
TdT$^{o/o}$ no. 2	15	8	tgtgctatgagaga		ccagggaggcagagctctg	**RDQGGRAL**	100
TdT$^{o/o}$ no. 3	15	8	tgtgctatgagaga		ccagggaggcagagctctg	**RDQGGRAL**	100
TdT$^{o/o}$ no. 4	15	8	tgtgctatgagaga		ccagggaggcagagctctg	**RDQGGRAL**	92
	13	8	tgtgctatgagag		caatttctgggacttaccag	RANSGTYQ	8

[a] Sequence occurence per total number of sequences, shown as a percentage number.

Discussion

Although we have clearly established a diminished TCR diversity in TdT-deficient mice compared with TdT$^{+/+}$ mice, the questions of 1) the role of TdT in the emergence of public T cell repertoires and 2) the structural and functional differences in the TCR of TdT$^{o/o}$ and TdT$^{+/+}$ mice remain to be examined. In attempts to answer these questions, we have studied the T cell responses of TdT$^{o/o}$ and TdT$^{+/+}$ mice to MHC class Ia- and MHC class II-restricted peptides and the public T cell repertoires of these two strains of mice in response to the selected epitopes were characterized.

We report in this work that public Vα-Jα and Vβ-Dβ-Jβ usage against three different epitopes presented by MHC class Ia or II molecules are strikingly conserved in TdT$^{o/o}$ mice. Furthermore, the C57BL/6 and TdT$^{o/o}$ CDR3 sequences are highly homologous. In addition, we found, by quantitative PCR on tetramer-positive T lymphocytes, that the percentages of public Vα segment usage for each peptide were similar in both strains of mice.

TdT$^{o/o}$ T cells gave good proliferative recall responses to the MHC class II-restricted epitopes, HBVc129–140 and Eα52–66 3Kp, albeit significantly reduced compared with those of TdT^{+} cells (Fig. 1*A*). Against HBVc129–140, Vα12-Jα27 and Vβ11-Jβ2.7 rearrangements are used in all TdT$^{o/o}$ and TdT$^{+/+}$ mice. For the Vα-Jα rearrangement, the public CDR3α sequences are closely similar, the D residue found in position 2 in the CDR3α of TdT$^{o/o}$ animals is replaced by G or E in C57BL/6 mice (Table II) and all CDR3α have the same length of 8 aa. Two CDR3β lengths are selected in C57BL/6 animals while in TdT$^{o/o}$ mice only the shorter CDR3β is found (Table I and Fig. 1*B*). This shortening of CDR3 is a characteristic feature of TdT$^{o/o}$ Vβ chains, as previously reported for double-positive CD3^{low} thymocytes and mature T lymphocytes (7, 32).

Shorter CDR3β (6 aa instead of 9 aa) is also observed in the Vβ6-Jβ2.7 rearrangement selected in TdT$^{o/o}$ T cells specific for the peptide Eα52–66 3Kp. In most CDR3β, M is found in position 2 in the long and short CDR3β. Interestingly, in 18 CDR3β of 21 (Table III) there is a D residue which may be strongly selected for by the Eα52–66 3Kp, reminiscent of the selection of positively charged residues (K or R) in the CDR3β of the MCC-specific TCR when the T residue from the antigenic MCC peptide is substituted by a glutamate (33). The crystallographic structure of the Eα54–66 3Kp peptide bound to IA^{b} showed that five amino acids at p1, p2, p3, p5, and p8 were TCR contact residues; in addition,

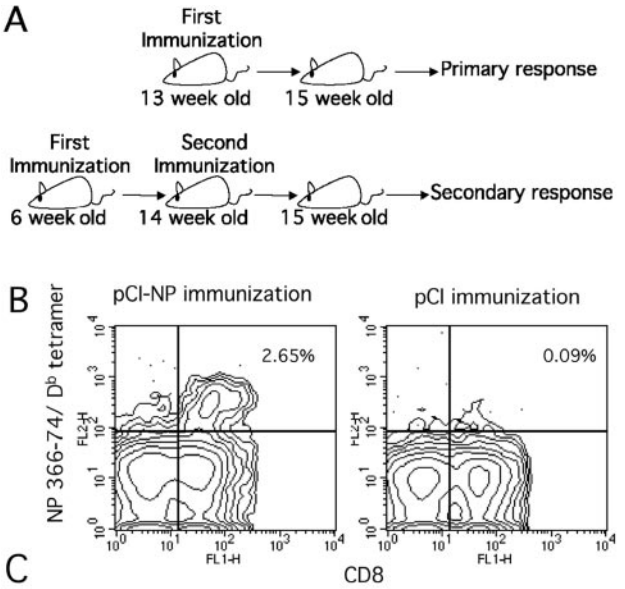

	C57Bl/6		TdT°/°	
	primary response	secondary response	primary response	secondary response
no. of studied mice	5	5	5	6
% of Tetramer positive cells	2±0.9	2.6±1.2	2.3±1.3	2.1±0.7
Mean Fluorescence Intensity	292±13	278±21	269±32	272±43

FIGURE 4. Flow cytometric analysis of NP influenza virus-specific T cells using D^{b}-NP366–74 tetramer for primary and secondary response in wild-type and TdT$^{o/o}$ animals. *A*, The schedule of immunization with the pCI-NP plasmid encoding the full-length NP of influenza virus is presented. *B*, Representative density plots of D^{b}-NP366–74 tetramer staining and CD8 expression are presented for a representative primary population following immunization. Splenocytes from pCI-NP plasmid encoding the full-length NP of the influenza virus-immunized mouse and the pCI plasmid-immunized mouse are labeled and analyzed on a flow cytometer. The percentage of CD8^{+}tetramer^{+} cells in all CD8^{+} cells is indicated. *C*, Comparison of percentages of CD8^{+} tetramer-positive cells and mean fluorescence intensity of tetramer staining after primary and secondary immunization in both strains of mice.

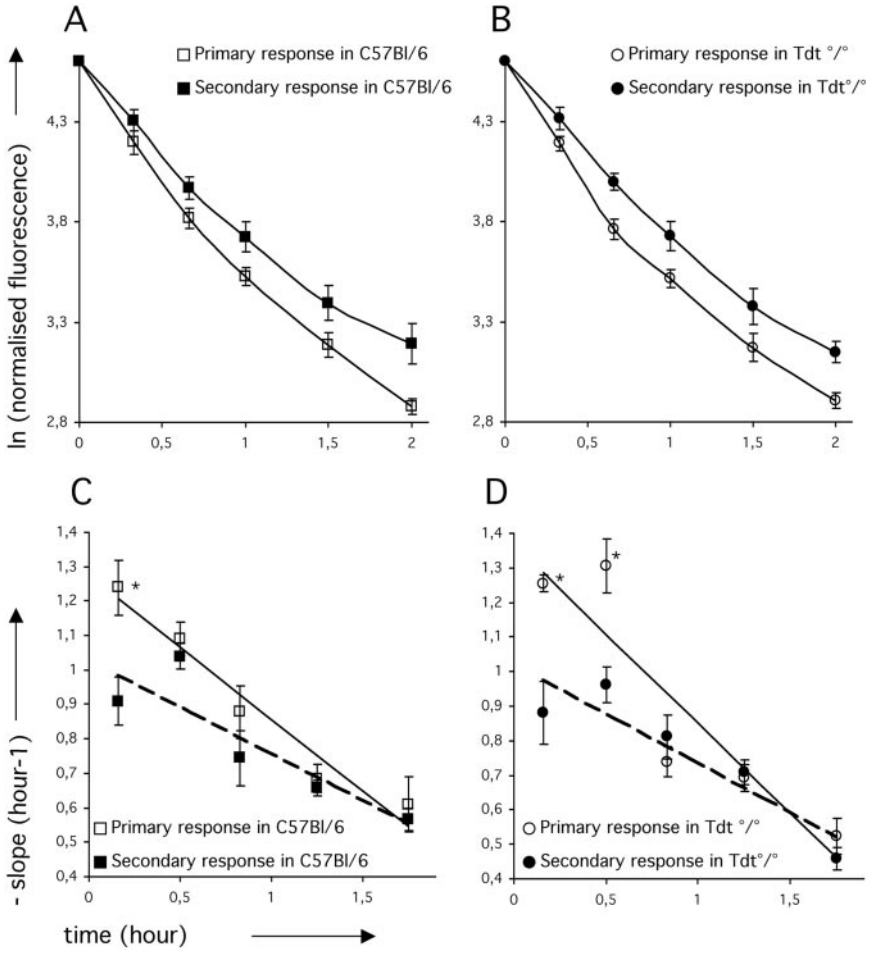

FIGURE 5. Tetramer staining decay kinetics for primary and secondary populations stained with D^b-NP366–74 tetramer. Tetramer staining decay plot of primary and secondary $CD8^+$ T cells from C57BL/6 (*A*) and $TdT^{o/o}$ mice (*B*). The natural logarithm of the normalized fluorescence is plotted vs time after addition of the unlabeled anti-D^b mAb KH95. Tetramer staining was evaluated at different times after KH95 addition. The normalized fluorescence (*f*) corresponds to the total fluorescence at a given time (*Fx*) divided by the total fluorescence at the initial time point (*F0*). The total fluorescence corresponds to the sum of the fluorescence intensities of D^b-NP366–74 tetramer-positive cells divided by the number of $CD8^+$ cells. Then, the ratio *ln* (*Fx*/*F0*) is plotted vs time. Quantitative analysis of tetramer staining decay kinescopes in wild-type mice (*C*) and in $TdT^{o/o}$ mice (*D*). For each time interval of the plots depicted in *A* and *B*, the mean slope of an interval is plotted vs the endpoint of that interval for primary and secondary T cells for wild-type and for TdT-deficient animals. The slope is equivalent to *ln* (*fa*/*fb*)/*t*, where *fa* is the normalized fluorescence at the start of the interval, *fb* the one at the end of the interval, and *t* is the length of the interval in hours. ∗, Statistically different ($p < 0.05$).

mutation of one of the three K completely abolished recognition by two specific T cell hybridomas (34). Thus, it is conceivable that the D residues found in the CDR3β form a salt bridge with one of the K residues of the antigenic peptide Eα52–66 3Kp. Concerning the Vα7-Jα13 used in response to Eα52–66 3Kp, the CDR3α sequence is identical in all TdT^+ and $TdT^{o/o}$ animals because it is generated by germline rearrangement of Vα7 and Jα13 segments. Interestingly, the CDR3α sequences SENYAQGL and SDNYAQGL are found in one C57BL/6 and two $TdT^{o/o}$ animals, respectively. It is possible that the presence of a glutamate residue in position 2 of SENYAQGL is selected for, because it is produced by N addition.

$TdT^{o/o}$ and $TdT^{+/+}$ CTLs generated in response to the MHC class I-restricted NP of influenza virus efficiently killed NP peptide-pulsed target cells. The Vβ public repertoire was homologous because the CDR3β sequences differed by one residue: A replaced S or G (Table V). The Vα public repertoire uses the same Vα-Jα rearrangement in both mouse strains, however, a CDR3 of 10 is selected in $TdT^{+/+}$ while a shorter CDR3 is found in $TdT^{o/o}$ mice. The consensus sequences were identified as RXSGGNAKL and as RDQGGRAL in C57BL/6 and $TdT^{o/o}$ mice, respectively. Interestingly, the public Vβ repertoire identified by Gavin and Bevan (6) in their collection of NP peptide-specific clones includes sequences SGGS/GNTGL (three clones of eight for C57BL/6) and SGGANTGQL (six clones of eight in $TdT^{o/o}$) (6). However, the public Vα repertoires could not be predicted from the CTL clones. The Immunoscope approach offers the advantage of allowing an easy identification of the Vβ and Vα repertoires against different epitopes (9, 10, 15, 17, 35) but cannot determine with certainty which Vβ and Vα are associated in T cell clones. The association of the CDR3α (RDGGRAL) and the CDR3β (SGGANTGQL), corresponding to the recurrent rearrangements in $TdT^{o/o}$ mice, was found in one CTL clone described by Gavin and Bevan (6). Interestingly, this clone is the most cross-reactive and detects 47 HPLC fractions from the H-$2D^b$-restricted peptide library (6).

Among the CTL clones produced by Gavin and Bevan (6), 50% of those derived from C57BL/6 use different Vβ-Jβ rearrangements and various Vα-Jα combinations. In contrast, most of the $TdT^{o/o}$ clones bear the same Vβ chains (six of eight). This decrease in diversity of the T cell repertoire in $TdT^{o/o}$ mice could lead to a lack of avidity maturation. The dissociation kinetics of NP-peptide/H-2 D^b tetramers bound to $CD8^+$ splenocytes from primary and secondary responses of C57BL/6 and $TdT^{o/o}$ mice (29) showed that avidity maturation occurs in both mouse strains but the large variations in staining decay, found in primary responses to MCC/I-E^k complexes in different mice, were not observed (29). In our model Ag, a statistically significant difference in avidity was observed between primary and secondary responses in both C57BL/6 and $TdT^{o/o}$ mice. The smaller individual variations observed may be due to the highly frequent T cell clones sharing TCRs of homogenous avidity for the NP peptide. Another possibility is that the recognition of this peptide/MHC complex by CTL is highly dependent on the CD8 molecule blurring differences in TCR affinity.

The recognition by individual $TdT^{o/o}$ CTL clones of a large panel of different MHC class I/antigenic peptide complexes has been reported by Gavin and Bevan (6) and these latter authors have suggested that TCR bearing no N additions interact predominantly

Table VII. *Statistical comparison of N nucleotides added in public and private β-chain rearrangements*

Ag	Seq	CDR3 Length	Vβ Usage	Jβ Usage	N	Total N Addition	
						μ	σ^2
Public							
HEL103–117	1	8	8.2	1.5	0		
HEL7–31	2	9	8.2	2.7	2.5		
HBVc129–140	4	7, 9	11	2.7	2		
SWM110–121	2	10	8.2	2.7	2.5		
P1A	1	9	1	1.2	3		
Cw3 170–179	3	6	10	1.2	2	1.64	0.94
MRL *lpr/lpr*	1	8	8.3	1.1	0		
P815E	1	9	1	2.5	1		
Ig Ck	3	7, 9	2, 6, 13	1.4, 2.3, 2.7	2		
PCC 88–103	6	9	3	1.2, 2.5	1.83		
NP 366–374	3	9	8.3	2.2	1.33		
Eα52–66 3 Kp	5	6, 9	6	2.7	1.6		
Private							
HEL 103–117	13	8–13	4, 6, 8.2	9 different	4.36		
HEL 7–31	3	8–12	8.1, 8.2, 14	1.5, 2.3, 2.7	3.33		
HBVc129–140	10	7–10	2, 4, 8.2, 8.3, 11, 13	1.1, 2.1, 2.3, 2.4, 2.7	3.4		
SWM110–121	20	7–11	8.2	1.4, 2.1, 2.2, 2.4, 2.5, 2.7	3.1	3.09	0.77
P1A	11	9	1	1.2	3		
Cw3 170–179	19	6	10	1.1, 1.2, 1.4, 2.3, 2.7	1.79		
FBL tumor	7	8–11	1, 3, 8.1, 14, 15	1.2, 2.1, 2.4, 2.5, 2.7	3.43		
NP 366–374	6	7–12	2, 5.1, 5.2, 8.1, 8.3	1.1, 1.6, 2.4, 2.7	2.33		
Average in total Vβ17 mouse T cell population					2.8		

with the MHC class I helices and less so with the peptides. This hypothesis is in agreement with the finding that a greater number of double-positive thymocytes undergoes positive selection than in $TdT^{+/+}$ mice (32).

Taking into consideration all these observations, we suggest that public repertoires bear the imprint of MHC molecules while private ones are more influenced or are selected by MHC bound self-peptides. Thus, three levels of complexity exist in the T cell repertoire: 1) the repertoire of neonates without N diversity and which interacts strongly with MHC molecules is thereby highly peptide cross-reactive; 2) the public repertoires which use the same V-J rearrangements as the neonatal ones and which include a moderate amount of N nucleotides and recognize a more restricted panel of antigenic peptides while keeping a good interaction with MHC molecules; and 3) the private repertoires which use distinct V-J combinations for each individual mouse and which contain a still larger proportion of N nucleotides (Table VII) in their CDR3 and interact in a highly specific way with the antigenic peptide and more weakly with the α helices of MHC molecules.

Several sets of experimental data suggest that CDR1 and CDR2/MHC interactions may play a predominant role in the selection of public repertoires. Single-site alanine mutagenesis of the 2C TCR has shown that CDR1 and CDR2 of Vα and Vβ chains contribute more to the binding energy with the MHC class I residues than CDR3s (36). Moreover, they estimated that two-thirds of the total energy is due to TCR residues interacting with MHCα helices. Studies of the interaction of the 2B4 TCR with MHC class II molecules complexed to a MCC peptide led to the two-step model of TCR recognition in which TCR/MHC interactions are required for association of the complex, while TCR/peptide contacts are involved mainly in stabilizing the complex (37). In the crystal structure of a public TCR bound to its cognate MHC-peptide, CDR2β contains five residues that interact with the HLA-B8 α1 helix and are found only in 2 of 54 human Vβ genes (Vβ7-8 and Vβ7-9). Finally, CDR1α and CDR2α residues from the Vα3.1 and Vα3.2 chains select preferentially $CD4^+$ or $CD8^+$ cells, presumably by stimulating interactions with either MHC class I or class II molecules (38). Overall, CDR1 and CDR2 interactions with MHC molecules are probably involved in positive selection in the thymus and are implicated in the generation of public repertoires, while CDR3 interactions may either favor negative selection or, in the case of long CDR3s, hinder positive selection.

Further studies in support of our hypothesis would necessitate the production of MHC class I molecules containing single mutations of the α helix amino acid residues with side chains interacting with the Vα or Vβ chains of the TCR to assess the effect of these mutations on the public repertoires in response to various epitopes.

Acknowledgments

We warmly thank Drs. P. Bousso, F. Lemonnier, B. Malissen, and D. Ojcius for their comments on the manuscript. We thank V. Mallier and A. Casrouge for hybridoma experiments.

References

1. Wilson, R. K., E. Lai, P. Concannon, R. K. Barth, and L. E. Hood. 1988. Structure, organization and polymorphism of murine and human T-cell receptor α and β chain gene families. *Immunol. Rev. 101:149*.
2. Lieber, M. 1992. The mechanism of V(D)J recombination: a balance of diversity, specificity and stability. *Cell 70:873*.
3. Gilfillan, S., A. Dierich, M. Lemeur, C. Benoist, and D. Mathis. 1993. Mice lacking TdT: mature animals with an immature lymphocyte repertoire. *Science 261:1175*.
4. Komori, T., A. Okada, V. Stewart, and F. W. Alt. 1993. Lack of N regions in antigen receptor variable region genes of TdT-deficient lymphocytes. *Science 261:1171*.
5. Bogue, M., S. Candeias, C. Benoist, and D. Mathis. 1991. A special repertoire of α:β T cells in neonatal mice. *EMBO J. 10:3647*.
6. Gavin, M. A., and M. J. Bevan. 1995. Increased peptide promiscuity provides a rationale for the lack of N regions in the neonatal T cell repertoire. *Immunity 3:793*.
7. Cabaniols, J. P., N. Fazilleau, A. Casrouge, P. Kourilsky, and J. M. Kanellopoulos. 2001. Most α/β T cell receptor diversity is due to terminal deoxynucleotidyl transferase. *J. Exp. Med. 194:1385*.
8. Gilfillan, S., M. Bachmann, S. Trembleau, L. Adorini, U. Kalinke, R. Zinkernagel, C. Benoist, and D. Mathis. 1995. Efficient immune responses in mice lacking N-region diversity. *Eur. J. Immunol. 25:3115*.
9. Cibotti, R., J. P. Cabaniols, C. Pannetier, C. Delarbre, I. Vergnon, J. M. Kanellopoulos, and P. Kourilsky. 1994. Public and private Vβ T cell receptor repertoires against hen egg white lysozyme (HEL) in nontransgenic versus HEL transgenic mice. *J. Exp. Med. 180:861*.
10. Levraud, J. P., C. Pannetier, P. Langlade-Demoyen, V. Brichard, and P. Kourilsky. 1996. Recurrent T cell receptor rearrangements in the cytotoxic T

lymphocyte response in vivo against the p815 murine tumor. *J. Exp. Med. 183:439*.

11. McHeyzer-Williams, M. G., and M. M. Davis. 1995. Antigen-specific development of primary and memory T cells in vivo. *Science 268:106*.
12. Cerasoli, D. M., M. P. Riley, F. F. Shih, and A. J. Caton. 1995. Genetic basis for T cell recognition of a major histocompatibility complex class II-restricted neoself peptide. *J. Exp. Med. 182:1327*.
13. Lehner, P. J., E. C. Wang, P. A. Moss, S. Williams, K. Platt, S. M. Friedman, J. I. Bell, and L. K. Borysiewicz. 1995. Human HLA-A0201-restricted cytotoxic T lymphocyte recognition of influenza A is dominated by T cells bearing the Vβ 17 gene segment. *J. Exp. Med. 181:79*.
14. Argaet, V. P., C. W. Schmidt, S. R. Burrows, S. L. Silins, M. G. Kurilla, D. L. Doolan, A. Suhrbier, D. J. Moss, E. Kieff, T. B. Suclley, et al. 1994. Dominant selection of an invariant T cell antigen receptor in response to persistent infection by Epstein-Barr virus. *J. Exp. Med. 180:2335*.
15. Gapin, L., Y. Bravo de Alba, A. Casrouge, J. P. Cabaniols, P. Kourilsky, and J. Kanellopoulos. 1998. Antigen presentation by dendritic cells focuses T cell responses against immunodominant peptides: studies in the hen egg-white lysozyme (HEL) model. *J. Immunol. 160:1555*.
16. Sourdive, D. J., K. Murali-Krishna, J. D. Altman, A. J. Zajac, J. K. Whitmire, C. Pannetier, P. Kourilsky, B. Evavold, A. Sette, and R. Ahmed. 1998. Conserved T cell receptor repertoire in primary and memory CD8 T cell responses to an acute viral infection. *J. Exp. Med. 188:71*.
17. Faure, M., S. Calbo, J. Kanellopoulos, A. M. Drapier, P. A. Cazenave, and D. Rueff-Juy. 1999. Tolerance to maternal immunoglobulins: resilience of the specific T cell repertoire in spite of long-lasting perturbations. *J. Immunol. 163:6511*.
18. Mikszta, J. A., L. J. McHeyzer-Williams, and M. G. McHeyzer-Williams. 1999. Antigen-driven selection of TCR in vivo: related TCR α-chains pair with diverse TCR β-chains. *J. Immunol. 163:5978*.
19. Rudolph, M. G., and I. A. Wilson. 2002. The specificity of TCR/pMHC interaction. *Curr. Opin. Immunol. 14:52*.
20. Housset, D., and B. Malissen. 2003. What do TCR-pMHC crystal structures teach us about MHC restriction and alloreactivity? *Trends Immunol. 24:429*.
21. Kjer-Nielsen, L., C. S. Clements, A. W. Purcell, A. G. Brooks, J. C. Whisstock, S. R. Burrows, J. McCluskey, and J. Rossjohn. 2003. A structural basis for the selection of dominant $\alpha\beta$ T cell receptors in antiviral immunity. *Immunity 18:53*.
22. Kjer-Nielsen, L., C. S. Clements, A. G. Brooks, A. W. Purcell, J. McCluskey, and J. Rossjohn. 2002. The 1.5 A crystal structure of a highly selected antiviral T cell receptor provides evidence for a structural basis of immunodominance. *Structure 10:1521*.
23. Motta, I., F. Andre, A. Lim, J. Tartaglia, W. I. Cox, L. Zitvogel, E. Angevin, and P. Kourilsky. 2001. Cross-presentation by dendritic cells of tumor antigen expressed in apoptotic recombinant canarypox virus-infected dendritic cells. *J. Immunol. 167:1795*.
24. Altman, J. D., P. A. H. Moss, P. J. R. Goulder, D. H. Barouch, M. G. McHeyzer-Williams, J. I. Bell, A. J. McMichael, and M. M. Davis. 1996. Phenotypic analysis of antigen-specific T lymphocytes. *Science 274:94*.
25. Bousso, P., A. Casrouge, J. D. Altman, M. Haury, J. Kanellopoulos, J. P. Abastado, and P. Kourilsky. 1998. Individual variations in the murine T cell response to a specific peptide reflect variability in naive repertoires. *Immunity 9:169*.
26. Rees, W., J. Bender, T. K. Teague, R. M. Kedl, F. Crawford, P. Marrack, and J. Kappler. 1999. An inverse relationship between T cell receptor affinity and antigen dose during CD4$^+$ T cell responses in vivo and in vitro. *Proc. Natl. Acad. Sci. USA 96:9781*.
27. Pannetier, C., M. Cochet, S. Darche, A. Casrouge, M. Zoller, and P. Kourilsky. 1993. The sizes of the CDR3 hypervariable regions of the murine T-cell receptor β chains vary as a function of the recombined germ-line segments. *Proc. Natl. Acad. Sci. USA 90:4319*.
28. Casrouge, A., E. Beaudoing, S. Dalle, C. Pannetier, J. Kanellopoulos, and P. Kourilsky. 2000. Size estimate of the $\alpha\beta$ TCR repertoire of naive mouse splenocytes. *J. Immunol. 164:5782*.
29. Savage, P. A., J. J. Boniface, and M. M. Davis. 1999. A kinetic basis for T cell receptor repertoire selection during an immune response. *Immunity 10:485*.
30. Busch, D. H., and E. G. Pamer. 1999. T cell affinity maturation by selective expansion during infection. *J. Exp. Med. 189:701*.
31. Fasso, M., N. Anandasabapathy, F. Crawford, J. Kappler, C. G. Fathman, and W. M. Ridgway. 2000. T cell receptor (TCR)-mediated repertoire selection and loss of TCR vβ diversity during the initiation of a CD4$^+$ T cell response in vivo. *J. Exp. Med. 192:1719*.
32. Gilfillan, S., C. Waltzinger, C. Benoist, and D. Mathis. 1994. More efficient positive selection of thymocytes in mice lacking terminal deoxynucleotidyl transferase. *Int. Immunol. 6:1681*.
33. Jorgensen, J. L., U. Esser, B. Fazekas De St. Groth, P. A. Reay, and M. M. Davis. 1992. Mapping T-cell receptor/peptide contacts by variant peptide immunization of single-chain transgenics. *Nature 355:224*.
34. Liu, X., S. Dai, F. Crawford, R. Fruge, P. Marrack, and J. Kappler. 2002. Alternate interactions define the binding of peptides to the MHC molecule IA^b. *Proc. Natl. Acad. Sci. USA 99:8820*.
35. Foucras, G., L. Gapin, C. Coureau, J. M. Kanellopoulos, and J. C. Guery. 2000. Interleukin 4-producing CD4 T cells arise from different precursors depending on the conditions of antigen exposure in vivo. *J. Exp. Med. 191:683*.
36. Manning, T. C., C. J. Schlueter, T. C. Brodnicki, E. A. Parke, J. A. Speir, K. C. Garcia, L. Teyton, I. A. Wilson, and D. M. Kranz. 1998. Alanine scanning mutagenesis of an $\alpha\beta$ T cell receptor: mapping the energy of antigen recognition. *Immunity 8:413*.
37. Wu, L. C., D. S. Tuot, D. S. Lyons, K. C. Garcia, and M. M. Davis. 2002. Two-step binding mechanism for T-cell receptor recognition of peptide MHC. *Nature 418:552*.
38. Sim, B. C., L. Zerva, M. I. Greene, and N. R. Gascoigne. 1996. Control of MHC restriction by TCR Vα CDR1 and CDR2. *Science 273:963*.